

Probing non-Hermitian phase transitions in curved space via quench dynamics

Ygor Pará,¹ Giandomenico Palumbo,² and Tommaso Macri^{1,3}

¹*Departamento de Física Teórica e Experimental,*

*Universidade Federal do Rio Grande do Norte, 59072-970 Natal-RN, Brazil**

²*School of Theoretical Physics, Dublin Institute for Advanced Studies, 10 Burlington Road, Dublin 4, Ireland[†]*

³*International Institute of Physics, Universidade Federal do Rio Grande do Norte, 59078-400 Natal-RN, Brazil[‡]*

(Dated: June 27, 2022)

Non-Hermitian Hamiltonians are relevant to describe the features of a broad class of physical phenomena, ranging from photonics and atomic and molecular systems, to nuclear physics and mesoscopic electronic systems. An important question relies on the understanding of the influence of curved background on the static and dynamical properties of non-Hermitian systems. In this work, we study the interplay of geometry and non-Hermitian dynamics by unveiling the existence of curvature-dependent non-Hermitian phase transitions. We investigate a prototypical model of Dirac fermions on a sphere with an imaginary mass term. This exactly-solvable model admits an infinite set of curvature-dependent pseudo-Landau levels. We characterize these phases by computing an order parameter given by the pseudo-magnetization and, independently, the non-Hermitian fidelity susceptibility. Finally, we probe the non-Hermitian phase transitions by computing the (generalized) Loschmidt echo and the dynamical fidelity after a quantum quench of the imaginary mass and find singularities in correspondence of exceptional radii of the sphere.

Introduction.—Non-Hermitian (NH) topological systems have become a very active and prolific research field in recent years [1–8]. This is due to their novel and peculiar physical features such as the NH skin effect [9–11] and the lacking of the conventional bulk-edge correspondence [12–17], as well as to the plethora of experimental platforms where these systems can be simulated and tested. A special class of non-Hermitian phases is defined by the \mathcal{PT} (parity and time reversal (TR)) symmetry, where the spectrum is completely real even with the absence of the Hermitian condition [18, 19]. This symmetry is important also because NH phase transitions are deeply related to the existence of the exceptional points (EPs) [20–24], which are associated to the critical phase transitions between \mathcal{PT} -symmetric and \mathcal{PT} -broken phases. These special points are characterized by topological invariants [25]. Moreover, the presence of EPs can be tested at dynamical level by employing genuine information-theoretic quantifiers such as (generalized) fidelities and Loschmidt echos [26–29]. Notice, these powerful theoretical tools have been largely used in the study of Hermitian phase transitions [30–45].

However, differently from Hermitian systems, the behavior of NH phases is still poorly understood on curved background. Curved space for emergent relativistic fermions in condensed matter physics can be associated, for instance, to the physical curvature of 1D, 2D and 3D materials, to effective geometry created from the synthetic matter or to formal geometric approaches employed to study the quantum thermal effects in topological phases [46–63]. Importantly, it has also been shown that curved background can give rise to genuine Hermitian phase transitions [64–67].

The main goal of our work is to unveil the existence of curvature-dependent non-Hermitian phase transitions.

These non-Hermitian phases are characterized by EPs which depend on the geometry of the system. In particular, these *geometric* EPs exist only on curved space and in general are hard to identify and describe due to the lack of translation symmetry. For this reason, we will present and study a prototypical analytical solvable model in two dimensions given by Dirac fermions on the sphere. This model has been already studied in the Hermitian case in the context of fullerene [68–74] and it also arises as a surface model of three-dimensional topological insulators [75–77]. We will induce NH phases by introducing an imaginary Dirac mass, which can be implemented by introducing on-site gain and loss as similarly to the flat case [7, 13, 78–81].

Firstly, we will analytically solve the model by showing the emergence of NH pseudo-Landau levels and their discrete symmetries. Notice, these pseudo-Landau levels are related to the intrinsic curvature of the sphere and are the analog of pseudo-Landau levels induced in flat space through strain [82–89].

Secondly, we will present the infinite sequence of geometric EPs, which will directly depend on the radius (curvature) of the sphere and relate the static properties of the spectrum through a pseudo-magnetization induced by the imaginary Dirac mass.

Finally, we will employ quench dynamics to characterize these curvature-dependent NH phase transitions. In particular, we will show that the NH versions of the Loschmidt echo and fidelity [29] are able to distinguish between the different phases of the model. The existence of non-analytic points in the fidelity will represent the clear signature of the presence of the geometric EPs. This will be performed by quenching the imaginary mass term and tuning the radius of the sphere to different values.

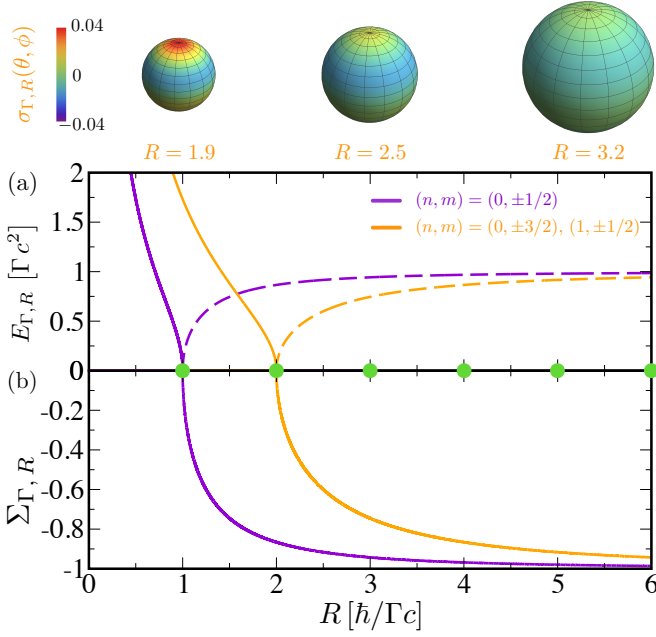


Figure 1. Eigenvalues and NH magnetization for the eigenstates of eq.(1) as a function of the radius R of the sphere. (a) $E_{\Gamma,R}$ for $\lambda = 1$ in units of Γc^2 for the first two pLLs with $(n, m) = (0, \pm 1/2)$ (purple) and $(1, \pm 1/2)$ (orange) in the TR-invariant region (real, full lines) and in the TR-broken phase (imaginary, dashed) according to eq.(3). At the EPs (green circles) the eigenvalues have vanishing energy, and eigenstates with opposite signs coalesce with degeneracy $d = 4\Omega_{nm}$. (b) $\Sigma_{\Gamma,R}$ from eq.(6) for $\lambda = 1$ and for the same pLLs of (a). At the EPs the spontaneous breaking of TR symmetry leads to a finite magnetization which asymptotically reaches the value $\Sigma_{\Gamma,\infty} = -1$. In the vicinity of the EPs $R \gtrsim R^*$, magnetization increases $\propto -\lambda(R - R^*)^{1/2}$. The energies and magnetizations for $\lambda = -1$ have opposite signs of $E_{\Gamma,R}$ and $\Sigma_{\Gamma,R}$. Top. Local magnetization $\sigma_{\Gamma,R}(\theta, \phi)$ across the EP at $R^* = 2$ for $(n, m, \lambda) = (1, 1/2, 1)$. For $R < R^*$, $\sigma_{\Gamma,R}(\theta, \phi) = -\sigma_{\Gamma,R}(\pi - \theta, \phi)$. For $R > R^*$, $\sigma_{\Gamma,R}(\theta, \phi)$ varies over a smaller range, and its integral is negative.

Model.—We consider the dynamics of relativistic fermions constrained to the surface of a sphere of radius R . The Dirac equation in 2+1 dimensions for a fermion of complex mass $\mu = M + i\Gamma$ (with both M and Γ real dimensionfull constants) in a curved background is described by a two-component spinor $\Psi(\mathbf{x})$ reads [90–93]

$$(i\hbar\bar{\gamma}^\nu\nabla_\nu + \mu c)\Psi(\mathbf{x}) = 0. \quad (1)$$

The space-time coordinates are labeled by $\mathbf{x} = (ct, \theta, \phi)$, the covariant derivative is given by $\nabla_\nu = \partial_\nu + \frac{1}{8}\omega_{\nu bc}[\gamma^b, \gamma^c]$. The spin connection $\omega_{\mu b}^d = e_\nu^d(e^\sigma_b\Gamma^\nu_{\sigma\mu} + \partial_\mu e^\nu_b)$ is written in terms of the metric connection $\Gamma^\nu_{\sigma\mu} = \frac{1}{2}g^{\beta\nu}(\partial_\mu g_{\sigma\beta} - \partial_\beta g_{\sigma\mu} + \partial_\sigma g_{\mu\beta})$. We are using a, b, \dots for local frame indices and μ, ν, \dots for coordinate indices. The metric of this space is $g_{\mu\nu} = \text{diag}(1, -R^2, -R^2 \sin^2 \theta)$, with determinant $g = R^4 \sin^2 \theta$. The vielbein is given by the definition $g_{\mu\nu} =$

$\eta_{ab}e_\mu^a e_\nu^b$, where $\eta_{ab} = \text{diag}(1, -1, -1)$. We also defined the inverse vielbein to satisfy $e_\mu^a e^{\mu}_b = \delta^a_b$. We write the gamma matrices as $\bar{\gamma}^\mu = e^\mu_a \gamma^a$, where we choose $\gamma^0 = \sigma_z$, $\gamma^1 = -i\sigma_x$, $\gamma^2 = -i\sigma_y$, consistently with the anti-commutation relations $\{\bar{\gamma}^\mu, \bar{\gamma}^\nu\} = 2g^{\mu\nu}$ [94].

The massless case represents the effective low-energy model for the some spherical condensed matter systems such as fullerene and the boundary states of spherical topological insulators [68–73, 75–77, 95–97]. It has also been employed in the prediction of some spectral properties related to the number of zero modes, which are theoretically predicted by the Atiyah-Singer index theorem [74, 98]. In the context of three-dimensional topological insulators, the model in eq.(1) displays several many-body phases in presence of attractive and in repulsive interactions [99].

By separating the time component from the spatial ones in eq. (1), we can write a Dirac Hamiltonian in the form

$$\hat{H}_\mu = \begin{pmatrix} -\mu c^2 & \frac{\hbar c}{R} \hat{h}^- \\ \frac{\hbar c}{R} \hat{h}^+ & \mu c^2 \end{pmatrix}, \quad (2)$$

with $\hat{h}^\pm = \pm(\partial_\theta + \frac{\cot\theta}{2}) + \frac{i}{\sin\theta}\partial_\phi$. It is important to note that due to the presence of the NH mass term $\hat{\Sigma}_z = -\mu c^2 \sigma_z$, eq.(2) is a NH Hamiltonian, i.e. $\hat{H}_\mu \neq \hat{H}_\mu^\dagger$. The eigenvalues $E_{\mu,R}^{(n,m,\lambda)}$ of H_μ can be obtained by squaring the Hamiltonian \hat{H}_μ of eq.(2)

$$E_{\mu,R}^{(n,m,\lambda)} = \lambda \sqrt{\frac{\hbar^2 c^2}{R^2} \Omega_{nm}^2 + \mu^2 c^4}, \quad (3)$$

where $\lambda = \pm 1$ and $\Omega_{nm} = n + |m| + 1/2$.

The indices n, m are respectively a positive integer and a half-integer, which label the pseudo-Landau levels (pLLs) of the model [100–103]. In the following we will focus on the case where the mass is purely imaginary, i.e. $\mu \equiv i\Gamma$. For this choice, an infinite set of EPs occur when $E_{\Gamma,R}^{(n,m,\lambda)} = 0$, i.e. $R\Gamma c^2 = \hbar c \Omega_{nm}$ with degeneracy $d = 4\Omega_{nm}$. At the EPs a pair of opposite-sign eigenvalues, connected by a square root branch point, coalesce [104, 105]. The evolution of the eigenvalues for the first pLLs are shown in fig.(1)a as a function of the sphere radius R . The EPs are located at $R = R^*$, with $R^* = 1, 2$ respectively. For $0 < R < R^*$ the eigenvalues are real, whereas for $R > R^*$ they are imaginary.

We notice that the two-component spinor eigenvectors $\phi_{\Gamma,R}^{(n,m,\lambda)}(\theta, \varphi)$ of \hat{H}_Γ have a nonvanishing scalar product

$$\int_0^\pi \int_0^{2\pi} \left(\phi_{\Gamma,R}^{(n_1,m_1,\lambda_1)}\right)^\dagger \phi_{\Gamma,R}^{(n_2,m_2,\lambda_2)} \sqrt{|g|} d\theta d\varphi = C_{\lambda_1,\lambda_2} \delta_{n_1,n_2} \delta_{m_1,m_2}, \quad (4)$$

with $C_{\lambda_1,\lambda_2} \neq 0$ for any nonzero value of Γ , and therefore they form a non-orthogonal basis [106, 107]. The prefactor of $\phi_{\Gamma,R}^{(n,m,\lambda)}(\theta, \varphi)$ is fixed by the requirement that the

normalization constant is unitary. See the supplemental material for a detailed derivation of the spectrum [108].

Discrete symmetries.—The parity operator, equivalent to space reflection in $2+1$ dimensions, can be written as $\mathcal{P} = \sigma_x P_\theta$, where P_θ takes $\theta \rightarrow \pi - \theta$. The TR operator is described by $\mathcal{T} = -i\sigma_y K$, where K is the usual complex conjugation. The massless Dirac Hamiltonian \hat{H}_0 in eq.(2) with $\Gamma = 0$ is Hermitian, and it is simultaneously invariant under the action of both the parity and TR symmetry [47, 76, 99, 109, 110]. Any finite (real or complex) mass breaks parity symmetry. Conversely, the Hamiltonian \hat{H}_Γ is invariant under TR symmetry. We also notice that, in our relativistic formulation, TR acts in a similar fashion as a combined $\mathcal{P}\mathcal{T}$ -symmetry for a single spin system with no center-of-mass dynamics [18]. The TR operator \mathcal{T} acts on the eigenstates $\phi_{\Gamma,R}^{(n,m,\lambda)}$ of \hat{H}_Γ as follows

$$\mathcal{T}\phi_{\Gamma,R}^{(n,m,\lambda)} = \begin{cases} (-1)^{m-\frac{1}{2}}\phi_{\Gamma,R}^{(n,-m,\lambda)} & \text{for } \hbar c\Omega_{nm} > R\Gamma c^2 \\ (-1)^{m-\frac{1}{2}}\phi_{\Gamma,R}^{(n,-m,-\lambda)} & \text{for } \hbar c\Omega_{nm} < R\Gamma c^2 \end{cases}. \quad (5)$$

Importantly, upon crossing any EPs, such that $R\Gamma c^2 > \hbar c\Omega_{nm}$ the effect of \mathcal{T} is to map an eigenstate $\phi_{\Gamma,R}^{(n,m,\lambda)}$ into an eigenstate $\phi_{\Gamma,R}^{(n,-m,-\lambda)}$ with opposite energy ($\lambda \rightarrow -\lambda$). Therefore an adiabatic variation of the radius (geometry) or the imaginary mass (gain-loss) across an EP *spontaneously* breaks TR symmetry.

Magnetic phases.—Based on the analysis of TR symmetry, and the analogy with usual magnetic systems, we expect the system to develop a spontaneous magnetization across an EP [111, 112]. Given a general spinor $\Phi = (\phi_\uparrow \ \phi_\downarrow)^T$ we define a NH magnetization as $\Sigma_{\Gamma,R} = \int_0^{2\pi} \int_{-1}^1 \sigma_{\Gamma,R}(\theta, \phi) \sqrt{|g|} d\theta d\phi$, where $\sigma_{\Gamma,R}(\theta, \phi) = (\phi_\uparrow^* \phi_\uparrow - \phi_\downarrow^* \phi_\downarrow)$ is the local magnetization (see top panel of fig.(1)) [99]. For an eigenstate $\phi_{\Gamma,R}^{(n,m,\lambda)}$ the NH magnetization can be computed analytically

$$\Sigma_{\Gamma,R}^{(n,m,\lambda)} = \frac{\frac{\hbar^2 c^2}{R^2} \Omega_{nm}^2 - \left| E_{\Gamma,R}^{(n,m,\lambda)} + i\Gamma c^2 \right|^2}{\frac{\hbar^2 c^2}{R^2} \Omega_{nm}^2 + \left| E_{\Gamma,R}^{(n,m,\lambda)} + i\Gamma c^2 \right|^2}. \quad (6)$$

In fig.(1)b we plot the magnetization for the pLL as a function of R . For $R < R^*$ the magnetization vanishes. At the critical radius $R = R^*$ the system develops a spontaneous magnetization. In the vicinity of an EP, with $R \gtrsim \hbar c\Omega_{nm}/\Gamma c^2$, we can expand eq.(6) to obtain

$$\Sigma_{\Gamma,R}^{(n,m,\lambda)} \Big|_{R \gtrsim R^*} \approx -\lambda \sqrt{2} \left(\frac{R - R^*}{R^*} \right)^{\frac{1}{2}}, \quad (7)$$

where $R^* = \hbar\Omega_{nm}/\Gamma c$ is the critical radius. Therefore the magnetization signals the presence a second-order phase transition with a critical exponent $\beta = 1/2$, analogous to the mean-field critical exponent of the (Hermitian) Ising transition. Asymptotically, for $R \rightarrow \infty$ the

magnetization saturates to $\Sigma_{\Gamma,\infty} = (-1)^\lambda$ depending on the sign of the energy eigenvalue. We emphasize that the NH magnetization $\Sigma_{\Gamma,R}^{(n,m,\lambda)}$ defined in eq.(6) relies on the use of the non-orthogonal basis $\{\phi_{\Gamma,R}^{(n,m,\lambda)}(\theta, \varphi)\}$ [113].

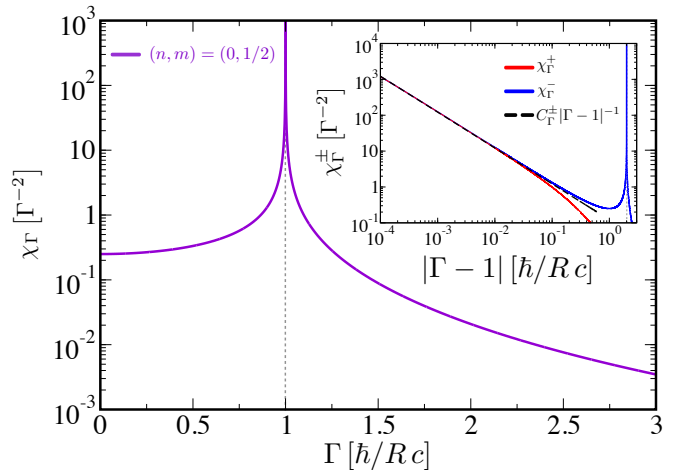


Figure 2. Fidelity susceptibility χ_Γ given by eq. (9) of the lowest pLL for $n = 0$ and $m = 1/2$, as function of the mass Γ . Susceptibility χ_Γ diverges at the EP $\Gamma^* = \hbar\Omega_{0,1/2}/Rc$. χ_Γ is a symmetric function of Γ , i.e. $\chi_\Gamma = \chi_{-\Gamma}$. Scaling of χ_Γ approaching the EP from the right (red line) and from the left (blue). Both susceptibilities were fitted with the function $\chi_\Gamma^\pm = C_\Gamma^\pm |\Gamma - \Gamma^*|^{-1}$, with $C_\Gamma^\pm = 0.122$. The second peak of χ_Γ^- corresponds to the EP at $\Gamma = -\hbar\Omega_{0,1/2}/Rc$ outside the scaling region of the inset.

Fidelity susceptibility.—A complementary approach to detect phase transitions *without* a previous knowledge of an order parameter is via the calculation of the fidelity susceptibility [30, 31, 33–36]. This approach has been recently generalized to the study of NH models [26–28]. Given two states $|\psi_{1,2}\rangle$, we define the NH fidelity is defined as [29]

$$\mathcal{F}_R\{|\psi_1\rangle, |\psi_2\rangle\} = \frac{|\langle \psi_1 | \psi_2 \rangle|^2}{\langle \psi_1 | \psi_1 \rangle \langle \psi_2 | \psi_2 \rangle}. \quad (8)$$

Notice that the scalar product $|\psi_{1,2}\rangle$ has to be computed at fixed radius R , whereas other parameters (such as the mass Γ or time t) can vary between the two states. The denominator in eq.(8) bounds the fidelity, $0 \leq \mathcal{F}_R \leq 1$. Given two states $|\psi_\Gamma\rangle$ and $|\psi_{\Gamma+\delta\Gamma}\rangle$, differing from an infinitesimal variation of the mass Γ one can define the nonorthogonal *static* fidelity susceptibility as

$$\chi_\Gamma = \lim_{\delta\Gamma \rightarrow 0} \frac{-\ln |\mathcal{F}_R\{|\psi_\Gamma\rangle, |\psi_{\Gamma+\delta\Gamma}\rangle\}|}{(\delta\Gamma)^2}. \quad (9)$$

In fig.(2) we plot χ_Γ for the lowest pLL with $(n, m, \lambda) = (0, 1/2, 1)$. The susceptibility satisfies $\chi_\Gamma = \chi_{-\Gamma}$ and diverges at the EP when $\Gamma = \hbar\Omega_{n,m}/Rc$. In the inset of fig.(2) we compute the scaling properties of χ_Γ

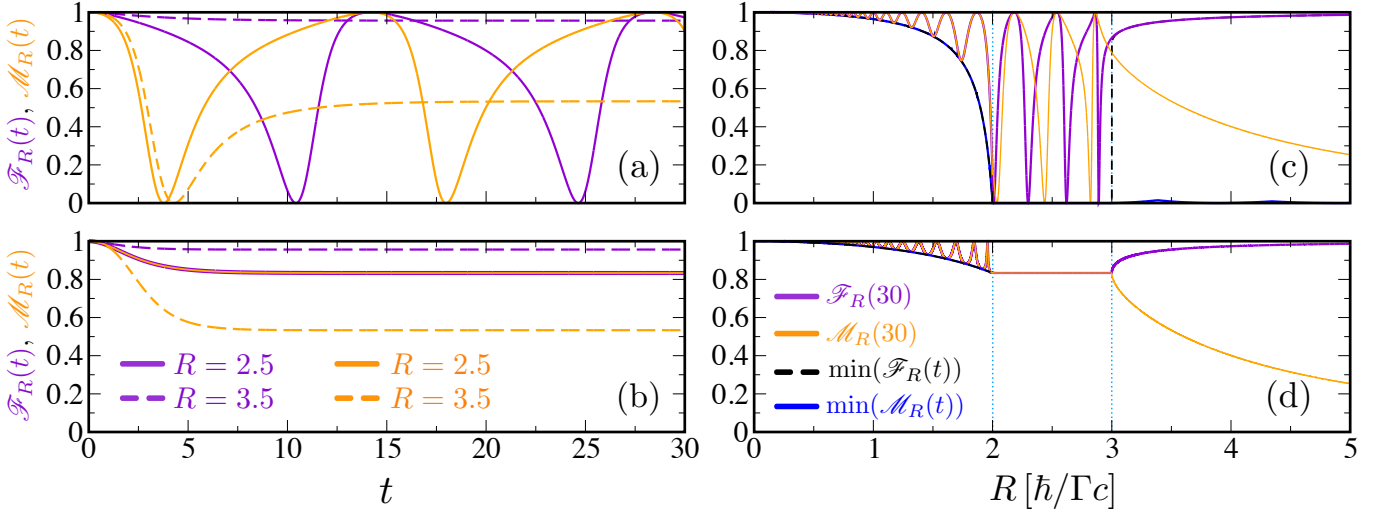


Figure 3. *Quench dynamics.* Fidelity $\mathcal{F}_R(t)$ (purple) and Loschmidt echo $\mathcal{M}_R(t)$ (orange) as a function of time (a)-(b) and as a function of the radius R (c)-(d) at $t = 30$ for two different mass quenches: (a) and (c) $\Gamma_i = 1/2$ and $\Gamma_f = 1/3$; (b) and (d) $\Gamma_i = 1/3$ and $\Gamma_f = 1/2$. For all cases we choose as the initial state the $|\psi_0\rangle = |\phi_{\Gamma_1,R}^{(n,m,\lambda)}\rangle$, the lowest pLL with $(n, m, \lambda) = (0, 1/2, 1)$ for the Hamiltonian \hat{H}_{Γ_i} .

around the EP at $\Gamma^* = 1$. Fitting the right (χ_{Γ}^+) and the left (χ_{Γ}^-) susceptibilities with the scaling functions $C_{\Gamma}^{\pm}|\Gamma - 1|^{\gamma}$ we find that $\gamma = 1$ with the same prefactor $C_{\Gamma}^{\pm} = 0.12$. Interestingly, we verified that the fidelity susceptibility has a qualitatively similar behavior adopting biorthogonal basis states. However the critical exponent γ is dependent on the choice of the basis states. Writing the generalized Uhlmann fidelity $F_{\Gamma} = (\langle \chi_{\Gamma+\delta\Gamma,R} | \psi_{\Gamma,R} \rangle \langle \chi_{\Gamma,R} | \psi_{\Gamma+\delta\Gamma,R} \rangle)^{1/2}$ computed on the eigenstates of \hat{H}_{Γ} and $\hat{H}_{\Gamma}^{\dagger}$ with the help of the biorthogonal basis [30], and computing the corresponding susceptibility $\chi_{\Gamma}^{(B)}$ [113], one obtains $\gamma = 2$ (see supplemental [108]).

Quench dynamics.—We investigate the quantum evolution after a mass quench in the proximity of EPs. We monitor the effect on the dynamics of a rapid variation of the mass from Γ_i to Γ_f via the (time-dependent) fidelity $\mathcal{F}_R(t)$ and the Loschmidt echo $\mathcal{M}_R(t)$ [29, 37]. The Loschmidt echo is a measure of the irreversibility suffered by the system during its evolution and generated by differences between forward and backward dynamics [38–43]. In contrast, the fidelity quantifies the deviation of the dynamics of a state induced by a perturbation. In NH systems, these perturbative effects are strongly increased in the proximity of the exceptional points [26]. We consider the case where the initial state, $|\psi_0\rangle = |\phi_{\Gamma_1,R}^{(n,m,\lambda)}\rangle$, is an eigenstate of \hat{H}_{Γ_1} , the case of a generic state can be obtained by an immediate generalization of this formalism. The Loschmidt echo is defined as [29]

$$\mathcal{M}_R(t) = \frac{|\langle \psi_0 | \psi_f(t) \rangle|^2}{\langle \psi_0 | \psi_0 \rangle \langle \psi_f(t) | \psi_f(t) \rangle}. \quad (10)$$

The initial state is propagated forward in time with the Hamiltonian \hat{H}_{Γ_1} and then time reversed and propagated backward in time with \hat{H}_{Γ_2} to obtain $|\psi_f(t)\rangle$. Exploiting the orthogonality relations among the eigenstates of the Dirac Hamiltonian for different masses $\Gamma_{1,2}$ (see [108]) the expression of the time-evolved state can be greatly simplified

$$|\psi_f(t)\rangle = \sum_{\bar{\lambda}=\pm} e^{i\frac{t}{\hbar}[E_{\Gamma_2,R}^{(n,m,\lambda)} - E_{\Gamma_1,R}^{(n,m,\lambda)}]} |\psi_{\Gamma_2,R}^{(n,m,\bar{\lambda})}\rangle \times \langle \chi_{\Gamma_2,R}^{(n,m,\bar{\lambda})} | \phi_{\Gamma_1,R}^{(n,m,\lambda)} \rangle. \quad (11)$$

Similarly, we compute the *time-dependent* fidelity $\mathcal{F}_R\{|\psi_1^{(\lambda)}(t)\rangle, |\psi_2^{(\lambda)}(t)\rangle\}$ defined in eq.(8) between the time-evolved initial state $|\phi_{\Gamma_1,R}^{(n,m,\lambda)}\rangle$ under \hat{H}_{Γ_1} , i.e

$$|\psi_1^{(\lambda)}(t)\rangle = e^{-i\frac{t}{\hbar}E_{\Gamma_1,R}^{(n,m,\lambda)}} |\phi_{\Gamma_1,R}^{(n,m,\lambda)}\rangle, \quad (12)$$

and \hat{H}_{Γ_2} , i.e.

$$|\psi_2^{(\lambda)}(t)\rangle = \sum_{\bar{\lambda}=\pm} e^{-i\frac{t}{\hbar}E_{\Gamma_2,R}^{(n,m,\lambda)}} |\psi_{\Gamma_2,R}^{(n,m,\bar{\lambda})}\rangle \langle \chi_{\Gamma_2,R}^{(n,m,\bar{\lambda})} | \phi_{\Gamma_1,R}^{(n,m,\lambda)} \rangle. \quad (13)$$

The Loschmidt echo and the fidelity evaluated on the eigenstates of eq.(1) satisfy the relation $\mathcal{F}_R^{(\lambda)}(t) = \mathcal{M}_R^{(-\lambda)}(t)$ [108]. Also, similarly to the Hermitian case, $\mathcal{F}_R^{(\lambda)}(t) = \mathcal{M}_R^{(\lambda)}(t)$ in the TR-invariant phase, whereas they generally differ in the TR-broken phase. In fig.(3) we plot the fidelity and the Loschmidt echo as a function of time and the radius R of the sphere for quenches where $\Gamma_i > \Gamma_f$ (figs.(a) and (c)) and $\Gamma_i < \Gamma_f$ (figs.(b) and (d))

with the initial state $|\phi_{\Gamma_1, R}^{(0,1/2,1)}\rangle$. For both $\Gamma_{i,f}$ we find two critical radii $R^* = 2$ and $R^* = 3$ (blue dotted lines) at which we observe singularities for $\min_{t \in [0, \infty[} \mathcal{F}_R(t)$ (black dashed lines) and $\min_{t \in [0, \infty[} \mathcal{M}_R(t)$ (blue line). For quenches within the TR-invariant region for both \hat{H}_{Γ_i} and \hat{H}_{Γ_f} , when $R < 2$, the fidelity and the Loschmidt echo coincides at all times, $\mathcal{F}_R(t) = \mathcal{M}_R(t)$, (c-d). When $2 < R < 3$ they are equivalent only when $\Gamma_i < \Gamma_f$ and it is independent of the radius, (b) and (d). At larger radii $R > 3$, $\mathcal{F}_R(t) > \mathcal{M}_R(t)$ for both quenches, (c) and (d). Notice that in this limit the small minimum value of the Loschmidt echo $\min_{t \in [0, \infty[} \mathcal{M}_R(t)$ in (c) is attained at intermediate times (dashed-orange curve in (a)), whereas in (d) it coincides with the asymptotic value $\mathcal{M}_R(\infty)$ (dashed-orange curve in (b)).

Conclusions.—In this work we have studied the influence of geometry in a prototypical problem of a Dirac particle moving on the surface of a sphere with an imaginary mass. From the analysis of the spectrum, we have found an infinite sequence of EPs arising from pLLs in the presence of an imaginary mass. The NH magnetization and fidelity susceptibilities reveal phase transitions in correspondence of the EPs from TR-invariant to TR-broken phases. Finally, we have investigated the quench dynamics through the Loschmidt echo and the fidelity and find singular behavior of these quantities at the EPs. Although our work is theoretical, nevertheless it paves the way to study and analyze curvature-dependent NH phases where the curved background can be experimentally realized in synthetic systems [98, 114–116]. Several branches of future investigation can be anticipated, such as the influence of hyperbolic geometry [115] and the introduction of topological defects [117] in NH phases.

Acknowledgements. We thank A. Lourenço for useful discussions. This study was financed in part by the Coordenação de Aperfeiçoamento de Pessoal de Nível Superior – Brasil (CAPES) – Finance Code 001. T.M. acknowledges CNPq for support through Bolsa de produtividade em Pesquisa n.311079/2015-6. This work was supported by the Serrapilheira Institute (grant number Serra-1812-27802), CAPES-NUFFIC project number 88887.156521/2017-00.

* ygpara@fisica.ufrn.br

† giandomenico.palumbo@gmail.com

‡ macri@fisica.ufrn.br

- [1] K. Esaki, M. Sato, K. Hasebe, and M. Kohmoto, *Phys. Rev. B* **84**, 205128 (2011).
- [2] Z. Gong, Y. Ashida, K. Kawabata, K. Takasan, S. Higashikawa, and M. Ueda, *Phys. Rev. X* **8**, 031079 (2018).
- [3] K. Kawabata, K. Shiozaki, M. Ueda, and M. Sato, *Phys. Rev. X* **9**, 041015 (2019).
- [4] E. J. Bergholtz, J. C. Budich, and F. K. Kunst, [arXiv:1912.10048](https://arxiv.org/abs/1912.10048) (2019).
- [5] V. M. Martinez Alvarez, J. E. Barrios Vargas, M. Berdakin, and L. E. F. Foa Torres, *Eur. Phys. J. Special Topics* **227**, 1295 (2018).
- [6] H. Zhou and J. Y. Lee, *Phys. Rev. B* **99**, 235112 (2019).
- [7] H. Shen, B. Zhen, and L. Fu, *Phys. Rev. Lett.* **120**, 146402 (2018).
- [8] J. M. Zeuner, M. C. Rechtsman, Y. Plotnik, Y. Lumer, S. Nolte, M. S. Rudner, M. Segev, and A. Szameit, *Phys. Rev. Lett.* **115**, 040402 (2015).
- [9] N. Okuma, K. Kawabata, K. Shiozaki, and M. Sato, *Phys. Rev. Lett.* **124**, 086801 (2020).
- [10] C. H. Lee and R. Thomale, *Phys. Rev. B* **99**, 201103 (2019).
- [11] S. Longhi, *Phys. Rev. Research* **1**, 023013 (2019).
- [12] F. K. Kunst, E. Edvardsson, J. C. Budich, and E. J. Bergholtz, *Phys. Rev. Lett.* **121**, 026808 (2018).
- [13] S. Yao, F. Song, and Z. Wang, *Phys. Rev. Lett.* **121**, 136802 (2018).
- [14] H. Wang, J. Ruan, and H. Zhang, *Phys. Rev. B* **99**, 075130 (2019).
- [15] S. Yao and Z. Wang, *Phys. Rev. Lett.* **121**, 086803 (2018).
- [16] D. S. Borgnia, A. J. Kruchkov, and R.-J. Slager, *Phys. Rev. Lett.* **124**, 056802 (2020).
- [17] K.-I. Imura and Y. Takane, *Phys. Rev. B* **100**, 165430 (2019).
- [18] C. M. Bender and S. Boettcher, *Phys. Rev. Lett.* **80**, 5243 (1998).
- [19] W. B. Rui, M. M. Hirschmann, and A. P. Schnyder, *Phys. Rev. B* **100**, 245116 (2019).
- [20] J. C. Budich, J. Carlström, F. K. Kunst, and E. J. Bergholtz, *Phys. Rev. B* **99**, 041406 (2019).
- [21] K. Kawabata, T. Bessho, and M. Sato, *Phys. Rev. Lett.* **123**, 066405 (2019).
- [22] T. Yoshida, R. Peters, N. Kawakami, and Y. Hatsugai, *Phys. Rev. B* **99**, 121101 (2019).
- [23] L. Zhou, Q.-h. Wang, H. Wang, and J. Gong, *Phys. Rev. A* **98**, 022129 (2018).
- [24] R. Arouca, C. H. Lee, and C. Morais Smith, [arXiv:2009.03541](https://arxiv.org/abs/2009.03541) (2020).
- [25] D. Leykam, K. Y. Bliokh, C. Huang, Y. D. Chong, and F. Nori, *Phys. Rev. Lett.* **118**, 040401 (2017).
- [26] Y.-C. Tzeng, C.-Y. Ju, G.-Y. Chen, and W.-M. Huang, (2020), [arXiv:2009.07070](https://arxiv.org/abs/2009.07070) [quant-ph].
- [27] G. Sun and S.-P. Kou, [arXiv:2009.11183](https://arxiv.org/abs/2009.11183) (2020).
- [28] N. Matsumoto, K. Kawabata, Y. Ashida, S. Furukawa, and M. Ueda, [arXiv:1912.09045](https://arxiv.org/abs/1912.09045) (2019).
- [29] S. Longhi, *Annalen der Physik* **531**, 1900054 (2019).
- [30] T. Gorin, T. Prosen, T. H. Seligman, and M. Žnidarič, *Physics Reports* **435**, 33 (2006).
- [31] S. T. Amin, B. Mera, C. Vlachou, N. Paunković, and V. R. Vieira, *Phys. Rev. B* **98**, 245141 (2018).
- [32] C. De Grandi, V. Gritsev, and A. Polkovnikov, *Phys. Rev. B* **81**, 012303 (2010).
- [33] P. Zanardi, P. Giorda, and M. Cozzini, *Phys. Rev. Lett.* **99**, 100603 (2007).
- [34] N. Paunković and V. Rocha Vieira, *Phys. Rev. E* **77**, 011129 (2008).
- [35] A. F. Albuquerque, F. Alet, C. Sire, and S. Capponi, *Phys. Rev. B* **81**, 064418 (2010).
- [36] S.-J. Gu, H.-M. Kwok, W.-Q. Ning, and H.-Q. Lin, *Phys. Rev. B* **77**, 245109 (2008).
- [37] T. Macrì, A. Smerzi, and L. Pezzè, *Phys. Rev. A* **94**,

- 010102 (2016).
- [38] A. Goussev, R. A. Jalabert, H. M. Pastawski, and D. A. Wisniacki, *Philosophical Transactions of the Royal Society A: Mathematical, Physical and Engineering Sciences* **374**, 20150383 (2016).
- [39] H. T. Quan, Z. Song, X. F. Liu, P. Zanardi, and C. P. Sun, *Phys. Rev. Lett.* **96**, 140604 (2006).
- [40] L. Campos Venuti and P. Zanardi, *Phys. Rev. A* **81**, 022113 (2010).
- [41] F. Pollmann, S. Mukerjee, A. G. Green, and J. E. Moore, *Phys. Rev. E* **81**, 020101 (2010).
- [42] R. Jafari and H. Johannesson, *Phys. Rev. Lett.* **118**, 015701 (2017).
- [43] B. Mera, C. Vlachou, N. Paunković, V. R. Vieira, and O. Viyuela, *Phys. Rev. B* **97**, 094110 (2018).
- [44] D. P. Pires, A. Smerzi, and T. Macrì, *Phys. Rev. A* **102**, 012429 (2020).
- [45] K. Macieszczak, E. Levi, T. Macrì, I. Lesanovsky, and J. P. Garrahan, *Phys. Rev. A* **99**, 052354 (2019).
- [46] F. de Juan, A. Cortijo, and M. A. H. Vozmediano, *Phys. Rev. B* **76**, 165409 (2007).
- [47] O. Boada, A. Celi, J. I. Latorre, and M. Lewenstein, *New Journal of Physics* **13**, 035002 (2011).
- [48] S. Ryu, J. E. Moore, and A. W. W. Ludwig, *Phys. Rev. B* **85**, 045104 (2012).
- [49] M. Stone, *Phys. Rev. B* **85**, 184503 (2012).
- [50] T. L. Hughes, R. G. Leigh, and O. Parrikar, *Phys. Rev. D* **88**, 025040 (2013).
- [51] G. Palumbo, R. Catenacci, and A. Marzuoli, *Int. J. Mod. Phys. B* **28**, 1350193 (2014).
- [52] A. Iorio and G. Lambiase, *Phys. Rev. D* **90**, 025006 (2014).
- [53] G. Palumbo and J. K. Pachos, *Ann. Phys.* **372**, 175 (2016).
- [54] C. Koke, C. Noh, and D. G. Angelakis, *Ann. Phys.* **374**, 162 (2016).
- [55] K. Landsteiner, Y. Liu, and Y.-W. Sun, *Phys. Rev. Lett.* **117**, 081604 (2016).
- [56] G. Palumbo, *Ann. Phys.* **386**, 15 (2017).
- [57] A. Celi, *The European Physical Journal Special Topics* **226**, 2729 (2017).
- [58] A. Westström and T. Ojanen, *Phys. Rev. X* **7**, 041026 (2017).
- [59] T. Kvorning, T. H. Hansson, A. Quelle, and C. M. Smith, *Phys. Rev. Lett.* **120**, 217002 (2018).
- [60] P. Maraner, J. K. Pachos, and G. Palumbo, *Scientific Reports* **9**, 17308 (2019).
- [61] J. Nissinen, *Phys. Rev. Lett.* **124**, 117002 (2020).
- [62] J. Nissinen and G. E. Volovik, *Phys. Rev. Research* **2**, 033269 (2020).
- [63] A. Farjami, M. D. Horner, C. N. Self, Z. Papić, and J. K. Pachos, *Phys. Rev. B* **101**, 245116 (2020).
- [64] T. Inagaki and K. Ishikawa, *Phys. Rev. D* **56**, 5097 (1997).
- [65] P. Gentile, M. Cuoco, and C. Ortix, *Phys. Rev. Lett.* **115**, 256801 (2015).
- [66] E. V. Castro, A. Flachi, P. Ribeiro, and V. Vitagliano, *Phys. Rev. Lett.* **121**, 221601 (2018).
- [67] Z. B. Siu, J.-Y. Chang, S. G. Tan, M. B. A. Jalil, and C.-R. Chang, *Scientific Reports* **8**, 16497 (2018).
- [68] A. A. Abrikosov Jr., arXiv e-prints, hep-th/0212134 (2002), arXiv:hep-th/0212134 [hep-th].
- [69] A. A. Abrikosov Jr, *Quantum field theory under the influence of external conditions. Proceedings, 5th Workshop, Leipzig, Germany, September 10-14, 2001*, *Int. J. Mod. Phys. A* **17**, 885 (2002), arXiv:hep-th/0111084 [hep-th].
- [70] D. V. Kolesnikov and V. A. Osipov, *The European Physical Journal B* **49**, 465 (2006).
- [71] J. González, F. Guinea, and M. A. H. Vozmediano, *Nuclear Physics B* **406**, 771 (1993).
- [72] M. Vozmediano, M. Katsnelson, and F. Guinea, *Physics Reports* **496**, 109 (2010).
- [73] R. Pincak, *Physics Letters A* **340**, 267 (2005).
- [74] J. K. Pachos, M. Stone, and K. Temme, *Phys. Rev. Lett.* **100**, 156806 (2008).
- [75] Y. Takane and K.-I. Imura, *Journal of the Physical Society of Japan* **82**, 074712 (2013), <https://doi.org/10.7566/JPSJ.82.074712>.
- [76] K.-I. Imura, Y. Yoshimura, Y. Takane, and T. Fukui, *Phys. Rev. B* **86**, 235119 (2012).
- [77] D.-H. Lee, *Phys. Rev. Lett.* **103**, 196804 (2009).
- [78] A. Szameit, M. C. Rechtsman, O. Bahat-Treidel, and M. Segev, *Phys. Rev. A* **84**, 021806 (2011).
- [79] Z.-Y. Ge, Y.-R. Zhang, T. Liu, S.-W. Li, H. Fan, and F. Nori, *Phys. Rev. B* **100**, 054105 (2019).
- [80] X. Ni, D. Smirnova, A. Poddubny, D. Leykam, Y. Chong, and A. B. Khanikaev, *Phys. Rev. B* **98**, 165129 (2018).
- [81] W. B. Rui, Y. X. Zhao, and A. P. Schnyder, *Phys. Rev. B* **99**, 241110 (2019).
- [82] H. Schomerus and N. Y. Halpern, *Phys. Rev. Lett.* **110**, 013903 (2013).
- [83] F. de Juan, J. L. Mañes, and M. A. H. Vozmediano, *Phys. Rev. B* **87**, 165131 (2013).
- [84] D. I. Pikulin, A. Chen, and M. Franz, *Phys. Rev. X* **6**, 041021 (2016).
- [85] S. Rachel, I. Göthel, D. P. Arovas, and M. Vojta, *Phys. Rev. Lett.* **117**, 266801 (2016).
- [86] A. G. Grushin, J. W. F. Venderbos, A. Vishwanath, and R. Ilan, *Phys. Rev. X* **6**, 041046 (2016).
- [87] G. Salerno, T. Ozawa, H. M. Price, and I. Carusotto, *Phys. Rev. B* **95**, 245418 (2017).
- [88] Z.-M. Huang, B. Han, and M. Stone, *Phys. Rev. B* **101**, 125201 (2020).
- [89] S. Laurila and J. Nissinen, arXiv:2007.10682 (2020).
- [90] R. M. Wald, *General Relativity* (Chicago Univ. Pr., Chicago, USA, 1984).
- [91] S. Weinberg, *Gravitation and Cosmology: Principles and Applications of the General Theory of Relativity* (John Wiley and Sons, New York, 1972).
- [92] M. Pollock, *Acta Phys. Polon. B* **41**, 1827 (2010).
- [93] P. Collas and D. Klein, *The Dirac Equation in Curved Spacetime* (Springer International Publishing, 2019).
- [94] M. Arminjon, *International Journal of Theoretical Physics* **54**, 2218 (2014).
- [95] J. González, F. Guinea, and M. A. H. Vozmediano, *Phys. Rev. Lett.* **69**, 172 (1992).
- [96] K. Yonaga, K. Hasebe, and N. Shibata, *Phys. Rev. B* **93**, 235122 (2016).
- [97] W.-H. Hsiao, *Phys. Rev. B* **101**, 155310 (2020).
- [98] B. Dietz, T. Klaus, M. Miski-Oglu, A. Richter, M. Bischoff, L. von Smekal, and J. Wambach, *Phys. Rev. Lett.* **115**, 026801 (2015).
- [99] T. Neupert, S. Rachel, R. Thomale, and M. Greiter, *Phys. Rev. Lett.* **115**, 017001 (2015).
- [100] M. Greiter and R. Thomale, *Annals of Physics* **394**, 33 (2018).

- [101] R. Ilan, A. G. Grushin, and D. I. Pikulin, *Nature Reviews Physics* **2**, 29 (2019).
- [102] M. Arciniaga and M. R. Peterson, *Phys. Rev. B* **94**, 035105 (2016).
- [103] P. Castro-Villarreal and R. Ruiz-Sánchez, *Phys. Rev. B* **95**, 125432 (2017).
- [104] C. M. Bender and S. Boettcher, *Phys. Rev. Lett.* **80**, 5243 (1998).
- [105] T. Kato, *Perturbation Theory for Linear Operators* (Springer Berlin Heidelberg, 1995).
- [106] M. Greiter, *Phys. Rev. B* **83**, 115129 (2011).
- [107] F. D. M. Haldane, *Phys. Rev. Lett.* **51**, 605 (1983).
- [108] see Supplemental Material.
- [109] X. Huang and L. Parker, *Phys. Rev. D* **79**, 024020 (2009).
- [110] R. Camporesi and A. Higuchi, *Journal of Geometry and Physics* **20**, 1 (1996).
- [111] B.-B. Wei and L. Jin, *Scientific Reports* **7** (2017), 10.1038/s41598-017-07344-z.
- [112] R. Streubel, P. Fischer, F. Kronast, V. P. Kravchuk, D. D. Sheka, Y. Gaididei, O. G. Schmidt, and D. Makarov, *Journal of Physics D: Applied Physics* **49**, 363001 (2016).
- [113] D. C. Brody, *Journal of Physics A: Mathematical and Theoretical* **47**, 035305 (2013).
- [114] N. Schine, A. Ryou, A. Gromov, A. Sommer, and J. Simon, *Nature* **534**, 671 (2016).
- [115] A. J. Kollár, M. Fitzpatrick, and A. A. Houck, *Nature* **571**, 45 (2019).
- [116] A. Greenleaf, Y. Kurylev, M. Lassas, and G. Uhlmann, *Phys. Rev. Lett.* **99**, 183901 (2007).
- [117] M. P. López-Sancho, F. de Juan, and M. A. H. Vozmediano, *Phys. Rev. B* **79**, 075413 (2009).
- [118] F. Kleefeld, (2009), arXiv:0906.1011 [hep-th].
- [119] F. Bagarello, R. Passante, and C. Trapani, eds., *Non-Hermitian Hamiltonians in Quantum Physics* (Springer International Publishing, 2016).
- [120] N. Moiseyev, *Non-Hermitian Quantum Mechanics* (Cambridge University Press, 2009).

SUPPLEMENTAL MATERIAL

A. Spectrum of the massive Dirac Hamiltonian

The eigenfunctions of \hat{H}_Γ are two-component spinors that satisfy the eigenvalue equation given by $\hat{H}_\Gamma \phi_{\Gamma,R}^{(m)}(\theta, \varphi) = E_{\Gamma,R}^{(m)} \phi_{\Gamma,R}^{(m)}(\theta, \varphi)$, where

$$\phi_{\Gamma,R}^{(m)}(\theta, \varphi) = \frac{e^{im\varphi}}{\sqrt{4\pi}} \begin{pmatrix} \alpha_{\Gamma,R}^{(m)}(\theta) \\ \beta_{\Gamma,R}^{(m)}(\theta) \end{pmatrix}, \quad (14)$$

with $m = \pm\frac{1}{2}, \pm\frac{3}{2}, \dots$

Now, we have

$$\frac{\hbar c}{R} \hat{h}^- \left[e^{im\varphi} \beta_{\Gamma,R}^{(m)}(\theta) \right] = \left(E_{\Gamma,R}^{(m)} + ic^2\Gamma \right) e^{im\varphi} \alpha_{\Gamma,R}^{(m)}(\theta); \quad (15a)$$

$$\frac{\hbar c}{R} \hat{h}^+ \left[e^{im\varphi} \alpha_{\Gamma,R}^{(m)}(\theta) \right] = \left(E_{\Gamma,R}^{(m)} - ic^2\Gamma \right) e^{im\varphi} \beta_{\Gamma,R}^{(m)}(\theta). \quad (15b)$$

These two equations combine, after a change of variables $\zeta = \cos \theta$, to give [68, 69]

$$\left[\frac{d}{d\zeta} (1 - \zeta^2) \frac{d}{d\zeta} - \frac{m^2 - \sigma_z m \zeta + 1/4}{1 - \zeta^2} + \Omega^2 - \frac{1}{4} \right] \begin{pmatrix} \alpha_{\Gamma,R}^{(m)}(\zeta) \\ \beta_{\Gamma,R}^{(m)}(\zeta) \end{pmatrix} = 0. \quad (16)$$

with

$$\Omega^2 = \frac{R^2}{\hbar^2 c^2} (E_m^2 + \Gamma^2 c^4). \quad (17)$$

Changing the variables as

$$\begin{pmatrix} \alpha_m(\zeta) \\ \beta_m(\zeta) \end{pmatrix} = \begin{pmatrix} (1 - \zeta)^{\frac{1}{2}|m-\frac{1}{2}|} (1 + \zeta)^{\frac{1}{2}|m+\frac{1}{2}|} \xi_m(\zeta) \\ (1 - \zeta)^{\frac{1}{2}|m+\frac{1}{2}|} (1 + \zeta)^{\frac{1}{2}|m-\frac{1}{2}|} \eta_m(\zeta) \end{pmatrix}, \quad (18)$$

one can verify

$$\left\{ (1 - \zeta^2) \frac{d^2}{d\zeta^2} + \left[\frac{m}{|m|} \sigma_3 - (2|m| + 2) \zeta \right] \frac{d}{d\zeta} + |m|(|m| + 1) + \left(\Omega_{nm}^2 - \frac{1}{4} \right) \right\} \begin{pmatrix} \xi_m(\zeta) \\ \eta_m(\zeta) \end{pmatrix} = 0. \quad (19)$$

For square integrable solutions [68] on the interval $x \in [-1, 1]$, we need that $\Omega_{nm}^2 = (n + |m| + \frac{1}{2})^2$, with non-negative integer $n \geq 0$.

Now, $\xi_{nm}(\zeta)$ and $\eta_{nm}(\zeta)$ are expressed in terms of the n -th order Jacobi polynomial as

$$\begin{pmatrix} \xi_{nm}(\zeta) \\ \eta_{nm}(\zeta) \end{pmatrix} = \begin{pmatrix} c_{nm}^\alpha P_n^{(|m-1/2|, |m+1/2|)}(\zeta) \\ c_{nm}^\beta P_n^{(|m+1/2|, |m-1/2|)}(\zeta) \end{pmatrix}. \quad (20)$$

From Eqs. (15) we find a condition to the coefficients

$$c_{\Gamma,R}^{\beta(n,m,\lambda)} = -\text{sgn}[m] \frac{\left[E_{\Gamma,R}^{(n,m,\lambda)} + ic^2\Gamma \right]}{\frac{\hbar c}{R} \Omega_{nm}} c_{\Gamma,R}^{\alpha(n,m,\lambda)}, \quad (21a)$$

$$c_{\Gamma,R}^{\alpha(n,m,\lambda)} = -\text{sgn}[m] \frac{\left[E_{\Gamma,R}^{(n,m,\lambda)} - ic^2\Gamma \right]}{\frac{\hbar c}{R} \Omega_{nm}} c_{\Gamma,R}^{\beta(n,m,\lambda)}. \quad (21b)$$

The absolute values of the constants can be found from the normalization conditions,

$$\int_0^{2\pi} \int_{-1}^1 \left[\phi_{nm}^{(\lambda)}(\zeta, \varphi) \right]^\dagger \phi_{nm}^{(\lambda)}(\theta, \varphi) R^2 d\zeta d\varphi = 1. \quad (22)$$

Therefore,

$$\left| c_{\Gamma,R}^{\alpha(n,m,\lambda)} \right| = \sqrt{\frac{\hbar^2 c^2 \Omega_{nm}^2 n!(n+2|m|)!}{R^2 2^{2|m|-1} \Gamma(\Omega_{nm})^2 R^2}} \sqrt{\frac{\hbar^2 c^2}{R^2} \Omega_{nm}^2 + \left| E_{\Gamma,R}^{(n,m,\lambda)} + ic^2\Gamma \right|^2}. \quad (23)$$

The eq. (14) becomes

$$\phi_{\Gamma,R}^{(n,m,\lambda)}(\zeta, \varphi) = c_{\Gamma,R}^{\alpha(n,m,\lambda)} a_{\Gamma,R}^{(n,m,\lambda)} \times \frac{e^{im\varphi}}{\sqrt{4\pi}} \begin{pmatrix} A_{nm}(\zeta) \\ -\frac{E_{\Gamma,R}^{(n,m,\lambda)} + i\Gamma c^2}{\text{sgn}[m] \frac{\hbar c}{R} \Omega_{nm}} B_{nm}(\zeta) \end{pmatrix}, \quad (24)$$

where

$$A_{nm}(\zeta) = \sqrt{1-\zeta}^{|m-\frac{1}{2}|} \sqrt{1+\zeta}^{|m+\frac{1}{2}|} P_n^{(|m-\frac{1}{2}|, |m+\frac{1}{2}|)}(\zeta), \quad (25a)$$

$$B_{nm}(\zeta) = \sqrt{1-\zeta}^{|m+\frac{1}{2}|} \sqrt{1+\zeta}^{|m-\frac{1}{2}|} P_n^{(|m+\frac{1}{2}|, |m-\frac{1}{2}|)}(\zeta), \quad (25b)$$

$$\text{and } a_{\Gamma,R}^{(n,m,\lambda)} = \sqrt{E_{\Gamma,R}^{(n,m,\lambda)} + i\Gamma c^2}^* / \left| \sqrt{E_{\Gamma,R}^{(n,m,\lambda)} + i\Gamma c^2} \right|.$$

The introduction of the term $a_{\Gamma,R}^{(n,m,\lambda)}$ will be useful for TR symmetry considerations.

B. Biorthogonal basis.

The eigenstates of \hat{H}_Γ satisfy $\hat{H}_\Gamma \psi_{nm}^{(\lambda)} = E_{nm}^{(\lambda)} \psi_{nm}^{(\lambda)}$. We now consider the Hamiltonian \hat{H}_Γ^\dagger given by

$$\hat{H}_\Gamma^\dagger = \begin{pmatrix} i\Gamma c^2 & \frac{\hbar c}{R} \hat{h}^- \\ \frac{\hbar c}{R} \hat{h}^+ & -i\Gamma c^2 \end{pmatrix}. \quad (26)$$

Also we have $H^\dagger \chi_{nm}^{(\lambda)} = \Xi_{nm}^{(\lambda)} \chi_{nm}^{(\lambda)}$. Note that the Hamiltonians H and H^\dagger differ only by the Γ signal. The eigenvalues of H and H^\dagger are related as $\Xi_{\Gamma,R}^{(n,m,\lambda)} = [E_{\Gamma,R}^{(n,m,\lambda)}]^*$. Therefore, the eigenvectors of H^\dagger are written as

$$\chi_{\Gamma,R}^{(n,m,\lambda)} = d_{\Gamma,R}^{\alpha(n,m,\lambda)} \frac{e^{im\varphi}}{\sqrt{4\pi}} \begin{pmatrix} A_{nm}(\zeta) \\ -\frac{[\Xi_{\Gamma,R}^{(n,m,\lambda)} - i\Gamma c^2]}{\text{sgn}[m] \frac{\hbar c}{R} \Omega_{nm}} B_{nm}(\zeta) \end{pmatrix}. \quad (27)$$

To define the bi-orthogonal basis appropriately [113, 118–120], we need to determine the constants $c_{\Gamma,R}^{\alpha(n,m,\lambda)}$ and $d_{\Gamma,R}^{\alpha(n,m,\lambda)}$ from of eqs. (14) and (27). From

$$\int_0^{2\pi} \int_{-1}^1 [\chi_{\Gamma,R}^{(n_1,m_1,\lambda_1)}]^\dagger \psi_{\Gamma,R}^{(n_2,m_2,\lambda_2)} R^2 d\zeta d\varphi = \delta_{n_1,n_2} \delta_{m_1,m_2} \delta_{\lambda_1,\lambda_2}, \quad (28)$$

we have,

$$\psi_{\Gamma,R}^{(n,m,\lambda)} = f_{\Gamma,R}^{(n,m,\lambda)} \frac{e^{im\varphi}}{\sqrt{4\pi}} \begin{pmatrix} A_{nm}(\zeta) \\ -\frac{[E_{\Gamma,R}^{(n,m,\lambda)} + i\Gamma c^2]}{\text{sgn}[m] \frac{\hbar c}{R} \Omega_{nm}} B_{nm}(\zeta) \end{pmatrix}, \quad (29)$$

$$\chi_{\Gamma,R}^{(n,m,\lambda)} = f_{\Gamma,R}^{(n,m,\lambda)*} \frac{e^{im\varphi}}{\sqrt{4\pi}} \begin{pmatrix} A_{nm}(\zeta) \\ -\frac{[\Xi_{\Gamma,R}^{(n,m,\lambda)} - i\Gamma c^2]}{\text{sgn}[m] \frac{\hbar c}{R} \Omega_{nm}} B_{nm}(\zeta) \end{pmatrix}, \quad (30)$$

where

$$f_{\Gamma,R}^{(n,m,\lambda)} = \sqrt{\frac{n!\Gamma(n+2|m|+1) \frac{\hbar^2 c^2 \Omega_{nm}^2}{R^2}}{2^{2|m|-1} \Gamma(\Omega_{nm})^2 R^2}}. \quad (31)$$

The relevant scalar products for different values of Γ for the states of eqs.(29) and (30) are given by

$$\langle \chi_{\Gamma_1,R}^{(\lambda_1)} | \psi_{\Gamma_2,R}^{(\lambda_2)} \rangle = \frac{f_{\Gamma_1,R}^{(n,m,\lambda_1)} f_{\Gamma_2,R}^{(n,m,\lambda_2)} R^2 2^{2|m|-1} \Gamma(\Omega_{nm})^2}{(\hbar^2 c^2 / R^2) \Omega_{nm}^2 n! \Gamma(n+2|m|+1)} \times \left(\frac{\hbar^2 c^2}{R^2} \Omega_{nm}^2 + [E_{\Gamma_1,R}^{(n,m,\lambda_1)} + i\Gamma_1 c^2] [E_{\Gamma_2,R}^{(n,m,\lambda_2)} + i\Gamma_2 c^2] \right) \quad (32)$$

and

$$\langle \psi_{\Gamma_1,R}^{(\lambda_1)} | \psi_{\Gamma_2,R}^{(\lambda_2)} \rangle = \frac{f_{\Gamma_1,R}^{(n,m,\lambda_1)} f_{\Gamma_2,R}^{(n,m,\lambda_2)} R^2 2^{2|m|-1} \Gamma(\Omega_{nm})^2}{(\hbar^2 c^2 / R^2) \Omega_{nm}^2 n! \Gamma(n+2|m|+1)} \times \left(\frac{\hbar^2 c^2}{R^2} \Omega_{nm}^2 + [E_{\Gamma_1,R}^{(n,m,\lambda_1)} + i\Gamma_1 c^2]^* [E_{\Gamma_2,R}^{(n,m,\lambda_2)} + i\Gamma_2 c^2] \right) \quad (33)$$

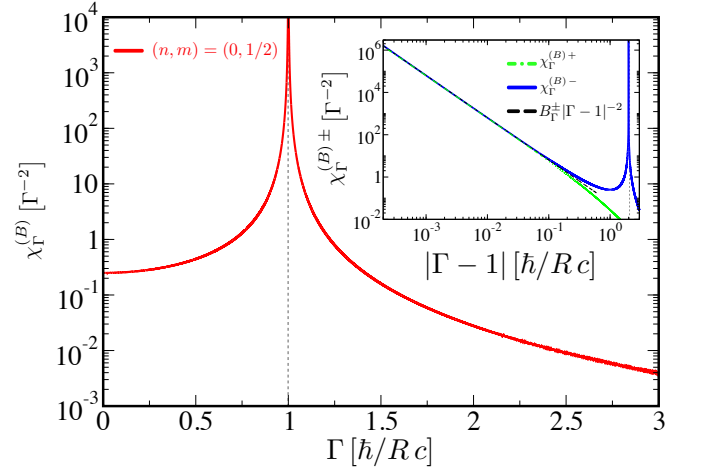


Figure 4. Biorthogonal fidelity susceptibility $\chi_\Gamma^{(B)}$ given by eq. (34) of the lowest pLL for $n = 0$ and $m = 1/2$, as function of the mass Γ . Susceptibility χ_Γ diverges at the EP $\Gamma^* = \hbar \Omega_{0,1/2}/Rc$. $\chi_\Gamma^{(B)}$ is a symmetric function of Γ , i.e. $\chi_\Gamma^{(B)} = \chi_{-\Gamma}^{(B)}$. Inset. Scaling of $\chi_\Gamma^{(B)}$ approaching the EP from the right (red line) and from the left (blue). Both susceptibilities were fitted with the function $\chi_\Gamma^{(B)\pm} = B_\Gamma^\pm |\Gamma - \Gamma^*|^{-2}$, with $B_\Gamma^\pm = 0.064$. The second peak of $\chi_\Gamma^{(B)-}$ corresponds to the EP at $\Gamma = -\hbar \Omega_{0,1/2}/Rc$ outside the scaling region of the inset.

1. Biorthogonal fidelity and susceptibility.

The fidelity susceptibility in the biorthogonal basis is defined as

$$\chi_\Gamma^{(B)} = \lim_{\delta\Gamma \rightarrow 0} \frac{-2 \ln |F_\Gamma|}{(\delta\Gamma)^2}, \quad (34)$$

where $F_\Gamma = (\langle \chi_{\Gamma+\delta\Gamma,R} | \psi_{\Gamma,R} \rangle \langle \chi_{\Gamma,R} | \psi_{\Gamma+\delta\Gamma,R} \rangle)^{1/2}$ is the generalized Uhlmann fidelity computed on the eigenstates of \hat{H}_Γ and \hat{H}_Γ^\dagger with the help of the biorthogonal basis [30].

The biorthogonal fidelity $F_\Gamma^{(B)}$ generalizes to the NH case the distance between two quantum states for different values of the mass Γ . In fig.(4) we plot $\chi_\Gamma^{(B)}$ for the lowest pLL of eq.(1) as a function of Γ . The susceptibility diverges at the EP and it is symmetric under the exchange $\Gamma \rightarrow -\Gamma$. In the inset of fig.(4) we show that $\chi_\Gamma^{(B)}$ diverges quadratically approaching the EP, i.e. $\chi_\Gamma^{(B)} \propto |\Gamma - \Gamma^*|^{-\gamma, \gamma'}$ with $\gamma = \gamma' = 2$ the right/left susceptibility critical exponents.

C. Quantum dynamics after a mass quench.

Given the state $|\phi_{\Gamma_1,R}^{(n,m,\lambda)}\rangle$ at $t = 0$, if $\hat{H}_{\Gamma_1,2}$ is independent of time, then its time evolution is $|\psi_1^{(\lambda)}(t)\rangle = e^{-i\frac{t}{\hbar}\hat{H}_{\Gamma_1,R}^{(n,m,\lambda)}}|\phi_{\Gamma_1,R}^{(n,m,\lambda)}\rangle$. In terms of the biorthogonal basis we can write $|\psi_{\Gamma_1,R}^{(n,m,\lambda)}\rangle = \sum_\ell |\psi_{\Gamma_2,R}^{(n,m,\ell)}\rangle \langle \chi_{\Gamma_2,R}^{(n,m,\ell)} | \phi_{\Gamma_1,R}^{(n,m,\lambda)}\rangle$, then $|\psi_2^{(\lambda)}(t)\rangle = \sum_\ell e^{-i\frac{t}{\hbar}E_{\Gamma_2,R}^{(n,m,\ell)}} |\psi_{\Gamma_2,R}^{(n,m,\ell)}\rangle \langle \chi_{\Gamma_2,R}^{(n,m,\ell)} | \phi_{\Gamma_1,R}^{(n,m,\lambda)}\rangle$. Computing the corresponding bras as

$$\langle \psi_1^{(\lambda)}(t) | = e^{itE_{\Gamma_1,R}^{(n,m,\lambda)*}} \langle \phi_{\Gamma_1,R}^{(n,m,\lambda)} |, \quad (35)$$

$$\langle \psi_2^{(\lambda)}(t) | = \sum_\ell e^{itE_{\Gamma_2,R}^{(n,m,\ell)*}} \langle \chi_{\Gamma_2,R}^{(n,m,\ell)} | \phi_{\Gamma_1,R}^{(n,m,\lambda)} \rangle^* \langle \psi_{\Gamma_2,R}^{(n,m,\ell)} |, \quad (36)$$

we define the fidelity $\mathcal{F}_R(t)$ as

$$\mathcal{F}_R(t) = \frac{|\langle \psi_1^{(\lambda)}(t) | \psi_2^{(\lambda)}(t) \rangle|^2}{\langle \psi_1^{(\lambda)}(t) | \psi_1^{(\lambda)}(t) \rangle \langle \psi_2^{(\lambda)}(t) | \psi_2^{(\lambda)}(t) \rangle}, \quad (37)$$

with

$$\begin{aligned} \langle \psi_1^{(\lambda)}(t) | \psi_2^{(\lambda)}(t) \rangle &= e^{i\frac{t}{\hbar}E_{\Gamma_1,R}^{(n,m,\lambda)*}} \sum_\ell e^{-i\frac{t}{\hbar}E_{\Gamma_2,R}^{(n,m,\ell)}} \times \\ &\times \langle \psi_{\Gamma_1,R}^{(n,m,\lambda)} | \psi_{\Gamma_2,R}^{(n,m,\ell)} \rangle \langle \chi_{\Gamma_2,R}^{(n,m,\ell)} | \psi_{\Gamma_1,R}^{(n,m,\lambda)} \rangle \end{aligned} \quad (38)$$

$$\begin{aligned} \langle \psi_2^{(\lambda)}(t) | \psi_2^{(\lambda)}(t) \rangle &= \sum_q \sum_\ell e^{i\frac{t}{\hbar}[E_{\Gamma_2}^{(q)*} - E_{\Gamma_2}^{(\ell)}]} \times \\ &\times \langle \chi_{\Gamma_2,R}^{(n,m,q)} | \psi_{\Gamma_1,R}^{(n,m,\lambda)} \rangle^* \langle \psi_{\Gamma_2,R}^{(n,m,q)} | \psi_{\Gamma_2,R}^{(n,m,\ell)} \rangle \times \\ &\times \langle \chi_{\Gamma_2,R}^{(n,m,\ell)} | \psi_{\Gamma_1,R}^{(n,m,\lambda)} \rangle, \end{aligned} \quad (39)$$

$$\langle \psi_1^{(\lambda)}(t) | \psi_1^{(\lambda)}(t) \rangle = e^{i\frac{t}{\hbar}[E_{\Gamma_1}^{(\lambda)*} - E_{\Gamma_1}^{(\lambda)}]} \langle \psi_{\Gamma_1,R}^{(n,m,\lambda)} | \psi_{\Gamma_1,R}^{(n,m,\lambda)} \rangle. \quad (40)$$

Note that we use the definition of $\psi_{\Gamma_2,R}^{(n,m,\ell)}$ normalized according to the bi-orthogonal basis, i.e., eq. (29).

Let us consider an initial state $|\psi_0^{(\lambda)}\rangle$ at time $t = 0$ an eigenstate of the \hat{H}_{Γ_1} , i.e., $|\psi_{\Gamma_1,R}^{(n,m,\lambda)}\rangle$. We make a temporal evolution in this state as $|\psi_f^{(\lambda)}\rangle = e^{i\frac{t}{\hbar}H_{\Gamma_2}} e^{-i\frac{t}{\hbar}H_{\Gamma_1}} |\psi_{\Gamma_1}^{(\lambda)}\rangle$

The Loschmidt echo $\mathcal{M}(t)$ is defined as

$$\mathcal{M}_R(t) = \frac{|\langle \psi_0^{(\lambda)} | \psi_f^{(\lambda)} \rangle|^2}{\langle \psi_0^{(\lambda)} | \psi_0^{(\lambda)} \rangle \langle \psi_f^{(\lambda)} | \psi_f^{(\lambda)} \rangle}, \quad (41)$$

with

$$\langle \psi_0^{(\lambda)} | \psi_f^{(\lambda)} \rangle = e^{-i\frac{t}{\hbar}E_{\Gamma_1}^{(\lambda)}} \sum_\ell e^{i\frac{t}{\hbar}E_{\Gamma_2}^{(\ell)}} \langle \psi_{\Gamma_1}^{(\lambda)} | \psi_{\Gamma_2}^{(\ell)} \rangle \langle \chi_{\Gamma_2}^{(\ell)} | \psi_{\Gamma_1}^{(\lambda)} \rangle, \quad (42)$$

$$\begin{aligned} \langle \psi_f^{(\lambda)} | \psi_f^{(\lambda)} \rangle &= e^{i\frac{t}{\hbar}[E_{\Gamma_1}^{(\lambda)*} - E_{\Gamma_1}^{(\lambda)}]} \sum_q \sum_\ell e^{i\frac{t}{\hbar}[E_{\Gamma_2}^{(\ell)} - E_{\Gamma_2}^{(q)*}]} \times \\ &\times \langle \chi_{\Gamma_2}^{(q)} | \psi_{\Gamma_1}^{(\lambda)} \rangle^* \langle \psi_{\Gamma_2}^{(q)} | \psi_{\Gamma_2}^{(\ell)} \rangle \langle \chi_{\Gamma_2}^{(\ell)} | \psi_{\Gamma_1}^{(\lambda)} \rangle, \end{aligned} \quad (43)$$

$$\langle \psi_0^{(\lambda)} | \psi_0^{(\lambda)} \rangle = \langle \psi_{\Gamma_1,R}^{(n,m,\lambda)} | \psi_{\Gamma_1,R}^{(n,m,\lambda)} \rangle. \quad (44)$$

Note also,

$$e^{-itE_{\Gamma_1}^{(\lambda)}} = \begin{cases} e^{-it\lambda\sqrt{\frac{\hbar^2c^2}{R^2}\Omega_{nm}^2 - \Gamma_1^2c^4}} & \text{if } \Gamma_1 < \Omega_{nm} \\ e^{t\lambda\sqrt{\Gamma_1^2c^4 - \frac{\hbar^2c^2}{R^2}\Omega_{nm}^2}} & \text{if } \Gamma_1 > \Omega_{nm} \end{cases} \quad (45)$$

$$e^{itE_{\Gamma_1}^{(\lambda)*}} = \begin{cases} e^{it\lambda\sqrt{\frac{\hbar^2c^2}{R^2}\Omega_{nm}^2 - \Gamma_1^2c^4}} & \text{if } \Gamma_1 < \Omega_{nm} \\ e^{-t\lambda\sqrt{\Gamma_1^2c^4 - \frac{\hbar^2c^2}{R^2}\Omega_{nm}^2}} & \text{if } \Gamma_1 > \Omega_{nm} \end{cases} \quad (46)$$

and

$$\langle \psi_{\Gamma_1}^{(\lambda)} | \psi_{\Gamma_2}^{(-\lambda)} \rangle = \langle \psi_{\Gamma_1}^{(-\lambda)} | \psi_{\Gamma_2}^{(\lambda)} \rangle^* \quad (47)$$

$$\langle \psi_{\Gamma_1}^{(\lambda)} | \psi_{\Gamma_2}^{(\lambda)} \rangle = \langle \psi_{\Gamma_1}^{(-\lambda)} | \psi_{\Gamma_2}^{(-\lambda)} \rangle \quad (48)$$

this implies that

$$\mathcal{F}_R^{(\lambda)}(t) = \mathcal{M}_R^{(-\lambda)}(t). \quad (49)$$

When $\lambda = 1$, with $\Gamma_1 > \Omega_{nm}$, $\Gamma_2 > \Omega_{nm}$ we have asymptotically ($t \rightarrow \infty$)

$$\mathcal{F}_R(t \rightarrow \infty) = \frac{|c_{\Gamma_2,\Gamma_1}^{(1,1)}|^2}{a_{\Gamma_2,\Gamma_1}^{(1,1,1)} \langle \psi_{\Gamma_1}^{(1)} | \psi_{\Gamma_1}^{(1)} \rangle}, \quad (50)$$

$$\mathcal{M}_R(t \rightarrow \infty) = \frac{|c_{\Gamma_2,\Gamma_1}^{(-1,1)}|^2}{\langle \psi_{\Gamma_1}^{(1)} | \psi_{\Gamma_1}^{(1)} \rangle b_{\Gamma_2,\Gamma_1}^{(-1,-1,1)}}, \quad (51)$$

where

$$a_{\Gamma_2,\Gamma_1}^{(q,\ell,\lambda)} = \langle \chi_{\Gamma_2}^{(q)} | \psi_{\Gamma_1}^{(\lambda)} \rangle^* \langle \psi_{\Gamma_2}^{(q)} | \psi_{\Gamma_2}^{(\ell)} \rangle \langle \chi_{\Gamma_2}^{(\ell)} | \psi_{\Gamma_1}^{(\lambda)} \rangle, \quad (52)$$

$$b_{\Gamma_2,\Gamma_1}^{(q,\lambda,\ell)} = \langle \chi_{\Gamma_2}^{(q)} | \psi_{\Gamma_1}^{(\lambda)} \rangle^* \langle \chi_{\Gamma_2}^{(\ell)} | \psi_{\Gamma_1}^{(\lambda)} \rangle, \quad (53)$$

$$c_{\Gamma_2,\Gamma_1}^{(\ell,\lambda)} = \langle \chi_{\Gamma_2}^{(\ell)} | \psi_{\Gamma_1}^{(\lambda)} \rangle^* \langle \psi_{\Gamma_2}^{(\ell)} | \psi_{\Gamma_1}^{(\lambda)} \rangle. \quad (54)$$

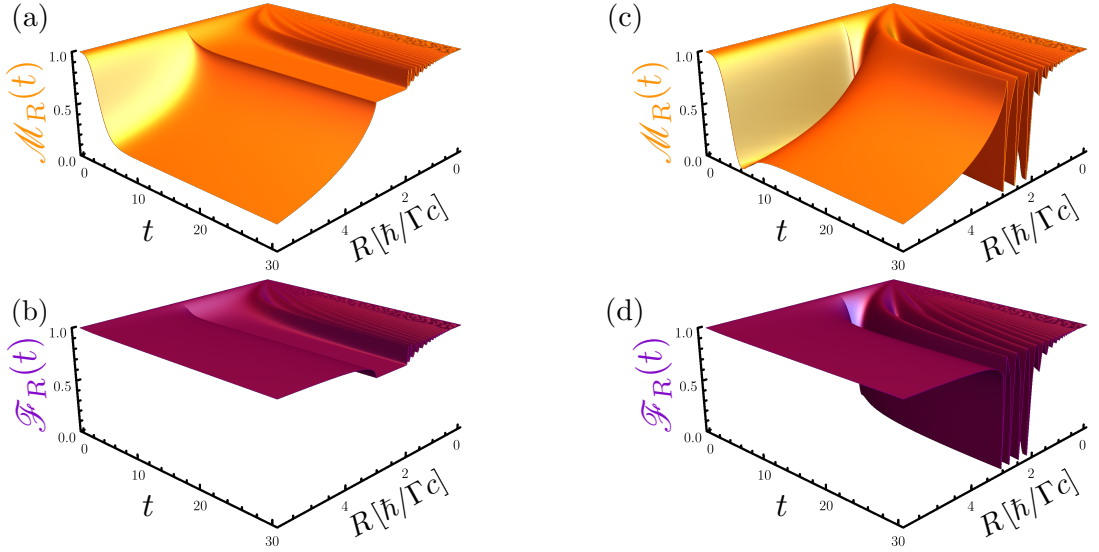


Figure 5. Three-dimensional plot of the fidelity $\mathcal{F}_R(t)$ (orange) and Loschmidt echo $\mathcal{M}_R(t)$ (purple) in function of the sphere radius R and time t for the mass quenches: (a) and (b) $\Gamma_i = 1/3$ and $\Gamma_f = 1/2$. (c) and (d) $\Gamma_i = 1/2$ and $\Gamma_f = 1/3$. For all cases we choose as the initial state the $|\psi_0\rangle = |\phi_{\Gamma_1, R}^{(n, m, \lambda)}\rangle$, the lowest pLL with $(n, m, \lambda) = (0, 1/2, 1)$ for the Hamiltonian \hat{H}_{Γ_i}

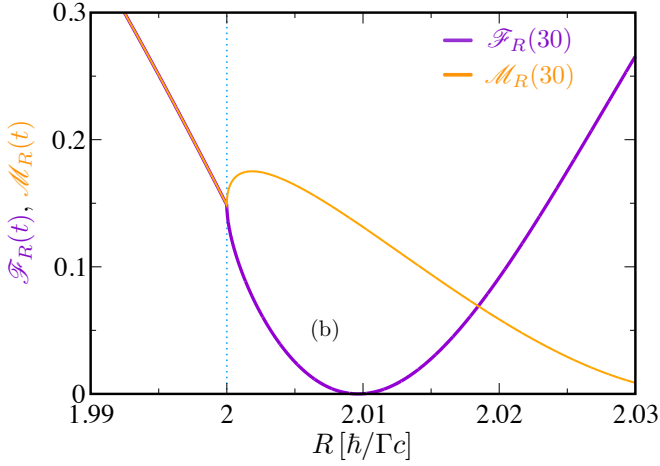


Figure 6. *Quench dynamics close to an EP.* Zoom of fig.(3)c for the fidelity $\mathcal{F}_R(t)$ (purple) and Loschmidt echo $\mathcal{M}_R(t)$ (orange) as a function of radius R at $t = 30$ for the mass quench with $\Gamma_i = 1/2$ and $\Gamma_f = 1/3$ close to an exceptional radius $R = 2$. For $R < 2$, $\mathcal{F}_R(t) = \mathcal{M}_R(t)$. At $R = 2$ they bifurcate and assume different values.

In fig.(5) we show the three-dimensional plot of $\mathcal{F}_R(t)$ and $\mathcal{M}_R(t)$ for the two quenches of fig.(3). In fig.(6) we zoom on the region around the EP at $R = 2$ where the fidelity and Loschmidt echo display a singularity and a bifurcation.